Modeling the Impact of Varying Black Carbon Concentrations on the Dielectric Properties and Radar Reflectivity of Arctic Sea Ice at Ka-Band Frequencies

Huzaifa Imran

[1]

***Abstract*—This study aims to model the impact that varying concentrations of Black Carbon (BC) can have on the dielectric properties and the radar reflectivity of Arctic sea ice specifically at Ka-Band frequencies (26.5-40GHz). For long, Black Carbon has been known to be an efficient radiation absorber and emitter which when deposited, can disrupt the energy balance by lowering the surface albedo of the Arctic Sea Ice. What is not discussed often, however, is the adverse effect of BC on radar systems monitoring Arctic sea ice. Radar systems are significant: they measure thickness, surface temperature, impurities, and reflectivity of the sea ice to monitor the Arctic Climate and subsequently predict global climate patterns. This study uses a new model that uses a combination of established data and formulae—including the Maxwell-Garnett Mixing Rule—to measure the aforementioned consequences of BC deposition, specifically its impact on the dielectric constant, attenuation coefficient, and radar reflectivity. This analysis revealed that an increase in the concentration of Black Carbon results in an increase in the effective dielectric constant of the Black Carbon-Sea Ice Composite, which in turn increases the attenuation coefficient which then decreases the Radar Reflectivity. The decrease in reflectivity was frequency-independent (within the Ka-Band), as all frequencies showed a similar reduction. It also revealed that Radar Reflectivity decreased with increasing frequencies, though this increase was not linear and varied for each frequency tested. The results of this investigation emphasize the dire need to incorporate BC deposition into satellite algorithms and models to improve the precision of environmental sensing. This study highlights the growing relevance of Black Carbon in disrupting radar monitoring systems and burgers further research into the complex electromagnetic behaviors of the particulate for the refinement of radar systems.**

***Index Terms*— Black Carbon (BC), dielectric constant, Ka-Band frequencies, Maxwell-Garnett Mixing Rule, Monte Carlo simulations, radar reflectivity, sea ice, satellite monitoring systems.**

I. INTRODUCTION

The Arctic plays a crucial role in global climate and geophysical observation systems. Its high surface albedo, which measures a surface's reflectivity, helps regulate global temperature by reflecting most of the incoming solar radiation [1]. This also makes the Arctic a key region for satellite communication and environmental monitoring. Moreover, its heightened vulnerability to climate change due to melting snow and ice makes it a critical area for studying climate dynamics and understanding the impacts of environmental changes. Unfortunately, in recent decades, the Arctic has experienced an unprecedented rate of warming, with temperatures rising at a rate nearly thrice that of the global average, in a phenomenon known as Arctic amplification [2]. This, due to the international relevance of the Arctic, has had profound implications on Earth's climate and Ecosystems [3], [4]; the economy [5]; and public health [6], [7].

Among the factors accelerating Arctic warming, the most efficient particulate species in the atmosphere to absorb visible light is Black Carbon (BC) [1]. Primarily generated from anthropogenic sources like the incomplete combustion of biomass, biofuels, and fossil fuels, as well as natural sources like wildfires, BC is the second most impactful emission in terms of its warming influence. Black carbon in the Arctic commonly exists as an aerosol and originates from various regions, including Eurasia and North America, transported via different circulation patterns [8]. BC, whether in the atmosphere or deposited on Arctic sea ice and snow, significantly impacts the region's energy balance—the equilibrium between the Sun's incoming energy and Earth's outgoing heat. Specifically, BC reduces the global mean precipitation, disrupts cloud dynamics, and deposits into the ocean, altering marine ecosystems [9]. More importantly, though, BC deposited on sea ice reduces albedo, causing the surface to absorb more heat and melt faster. This melting exposes darker ocean surfaces, further lowering albedo and creating a positive feedback loop that accelerates warming. This effect of BC on sea ice's albedo is shown in Fig. 1.

[1]First Author Huzaifa Imran is with the Roots IVY International School, Lahore (e-mail: huzaifaimranashraf12@gmail.com).

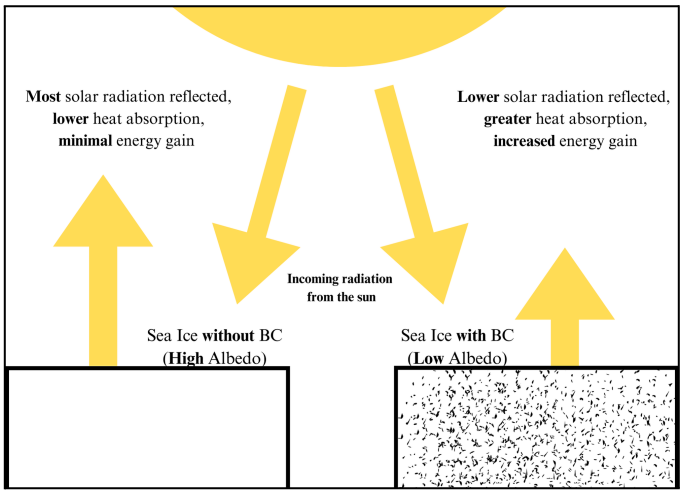

Fig. 1. Albedo comparison of Sea Ice with and without Black Carbon: The presence of Black Carbon darkens the surface, resulting in lower albedo, and hence lower solar radiation being reflected.

Beyond these direct climatic effects, the presence of BC also poses significant challenges for the very systems used to monitor these environmental changes, particularly satellite-based observation and communication systems [10]. Given the Arctic's critical role in environmental monitoring, it is important not to overlook the impacts of BC on Radar Reflectivity and satellite monitoring. Satellites, such as those utilizing high-frequency radar systems, are crucial in monitoring the Arctic environment by providing real-time data on ice thickness, sea ice extent, and surface temperatures [11]. Data from these satellites equips local communities and policymakers with essential knowledge about environmental shifts, such as permafrost thawing (ice inside permafrost melts to leave water and soil) and biodiversity loss, which are exacerbated by climate change [12].

Climate forcers like BC bring about significant challenges in satellite monitoring through deposition on the Arctic sea ice. As discussed earlier, BC enhances the absorption of solar radiation, reducing the radiation that is reflected in space [2]. This happens because BC can alter the electromagnetic properties of the ice, specifically its dielectric constant, which measures how well a material can store electrical energy when exposed to an electric field. Changes in the dielectric constant affect how radar signals interact with the ice surface, impacting the accuracy of radar measurements.

We hypothesize that an increase in the concentration of deposited BC increases the dielectric constant of Arctic sea ice across all tested frequency bands (28-40 GHz, every GHz), in turn causing a decrease in radar reflectivity. This reduction in signal strength could result in decreased accuracy of satellite-based observations, disrupting effective monitoring and communication systems in the Arctic region. Previous research has noted significant discrepancies in BC measurements due to different methods, resulting in high uncertainty. That, and the limited understanding of BC's effects on sea ice's electromagnetic properties across microwave frequencies underscores the need for this study.

We aim to model the impact of a range of BC concentrations (0-30%, every 5%) on the dielectric properties of arctic sea ice and radar reflectivity at different frequencies within the Ka-Band using Python libraries such as Matplotlib and Pandas. Through analyzing these relationships, we'll contribute to the reliability of satellite monitoring systems and promote informed decisions in climate policy and preservation efforts. The following sections will include a comprehensive review of past and contemporary literature, outline the methods for modeling radar reflectivity, present the results of varying BC concentrations, and discuss the broader implications for Arctic climate monitoring.

II. LITERATURE REVIEW

A. Introduction to Black Carbon (BC) & its Role in Climate Change

Commonly known as soot, Black Carbon (BC) is a tiny, carbonaceous component of fine particulate matter ($PM_{2.5}$)–the combination of all solid and liquid particles that are often hazardous and ≤ 2.5 microns in diameter suspended in the air. The particle, which is insoluble in water and common organic solvents [1], is formed as a result of the incomplete combustion of biomass, such as in brick kilns, coke ovens, wildfires, burning of agricultural residue, waste burning, and coal; and fossil fuels, including diesel engines, gasoline-powered vehicles, and ships [13]. It is also important to note that sources of black carbon emissions differ between the seasons. For example, in winter, anthropogenic sources like domestic burning of biomass, are significant contributors to atmospheric black carbon concentrations. In the summer, however, wildfires become a major source of black carbon emissions [14], [2].

Due to few sources of pollution within the Arctic, almost all BC found there is transported from mid-latitudes. The exact transportation routes of BC are discussed in [15] as heavily influenced by the region's meteorology, leading to different spatial patterns. BC aerosols accumulate during the transition between winter and spring, leading to a phenomenon known as the Arctic haze–an apparent haze in the Arctic atmosphere as resultants of anthropogenic pollution transport there. The haze results from the winds originating from central Asia and eastern Siberia which transport BC to the eastern part of the Arctic Sea where it accumulates, increasing in concentration. In the summer, as discussed before, smoke from forest fires is a significant contributor as mentioned in [8], and travels long distances from Eurasia and North America. The western part of the sea, even in the summer, exhibits lower BC concentrations as winds in this region flow from the sea towards Alaska, impeding any transport from the wildfires to this area.

Per [16], Black Carbon (BC) could be responsible for more than 30% of the warming observed in the Arctic, making it a primary danger to climate stability and environmental sustainability. BC influences the climate in two main ways. First, BC aerosols efficiently absorb radiation; they take in sunlight and other types of radiation, convert it into heat energy, and release it into the atmosphere. This process significantly contributes to radiative forcing, the imbalance between the incoming and outgoing energy, and disrupts the energy balance as more heat is retained in the atmosphere. Secondly, when BC settles on Arctic sea ice, it darkens the ice surfaces, reducing their albedo. Lower albedo means that less solar radiation is being reflected into space and more is being absorbed by the ice, leading to higher surface temperatures and accelerated melting of snow and sea ice. This stimulated melting not only contributes to rising sea levels but also reduces the region's capacity to reflect solar energy effectively, reinforcing a feedback loop where the Arctic warms faster than the global average. Moreover, the synergistic effect of BC with other climate forcers such as CO_2 causes a cumulative warming effect which furthers the effects of arctic amplification.

A key factor to consider when discussing the implications and subsequent solutions of BC on climate change is its lifetime. Reference [17] quotes the global mean lifetime of BC aerosol in the Arctic as 5.5 days while [18] suggests that Arctic-deposited BC lasts 37-232 days. This is negligible to the average millennium arctic atmospheric lifetime of CO_2 stated in [19]. This is important because, due to BC's short atmospheric lifetime, reducing its emissions would lead to immediate improvements in environmental quality, whereas CO_2 emissions would remain detrimental for years afterward.

B. Electromagnetic properties of Sea Ice

Despite the rising international concern of Black Carbon Deposition in the Arctic and its well-established effects on sea ice albedo and melt rates, there remains a scarcity of literature on how BC directly influences the electromagnetic properties of sea ice. Therefore, in this study, we will take the approach of first understanding the electromagnetic properties of Arctic sea ice and then the subsequent effects caused by BC deposition. Before moving forward, we must know that Permittivity is a fundamental material property that quantifies the ability to store electrical energy in an electric field.

When we talk about electromagnetic properties in this context, it is most important to consider the dielectric constant. Also known as relative permittivity, the dielectric constant is a dimensionless constant that describes how a material behaves in an electric field compared to a vacuum. It provides the mathematical representation of a material's response to an electric field and its ability to store electrical energy in that field [11]. Throughout this paper, we will be using the dielectric constant and relative permittivity interchangeably though they have some minor differences. The dielectric constant acts as the fundamental parameter for describing the interaction of electromagnetic waves with sea ice. Equation (1) shows how the dielectric constant is computed, and (2) shows the components of the relative permittivity.

$$\kappa = \epsilon_r = \frac{\epsilon}{\epsilon_0} \tag{1}$$

$$\epsilon_r = \epsilon' - j\epsilon'' \tag{2}$$

Equation (1) defines the ratio of the dielectric constant specifically stating that relative permittivity ϵ_r is equal to the ratio of the absolute permittivity of the material ϵ (the ability of the material to permit electric field lines) and the constant vacuum permittivity ϵ_0 representing the permittivity of free space.

More importantly, (2) describes the components of the dielectric constant namely the real (ϵ') and imaginary (ϵ'') components. For the scope of this research, it is key to understand what these components represent. ϵ' represents a material's ability to store electrical energy while ϵ'' representing its ability to dissipate it. Considering this, we can develop an equation (3) for the loss tangent.

$$tan\delta = \frac{\epsilon''}{\epsilon'} \tag{3}$$

Loss Tangent (tanδ) quantifies the dielectric loss in a material, representing the ratio of the imaginary part (ϵ'') to the real part (ϵ') of the relative permittivity (ϵ_r). It indicates how much electromagnetic energy is dissipated as heat within the material. This quantity is crucial in understanding the effects that BC may have on sea ice when it alters its dielectric properties.

Loss Tangent (tanδ) quantifies the dielectric loss in a material, representing the ratio of the imaginary part (ϵ'') to the real part (ϵ') of the relative permittivity (ϵ_r). It indicates how much electromagnetic energy is dissipated as heat within the material. This quantity is crucial in understanding the effects that BC may have on sea ice when it alters its dielectric properties.

Carrying out this investigation boils down to understanding the factors that influence the dielectric constant, the value determining the electromagnetic interaction of sea ice. Sea ice contains brine inclusions (pockets of concentrated salty water that get trapped within sea ice during the freezing process) trapped within the ice matrix.

These inclusions are crucial, determining the electromagnetic properties of sea ice through their influence on the scattering of electromagnetic radiation htiting the sea ice [20]. The complete effect of brine inclusions is complicated. On one hand, increased brine volume enhances the ability of sea ice to store electrical energy, increasing the real (ϵ') part of the dielectric constant, and leading to a higher constant overall.

Contrary to this, dissolved ions in increased brine volume increase conductivity, leading to higher dielectric loss, increasing the imaginary (ϵ'') part of the dielectric constant. According to (2), an overall increase in the dielectric constant is associated with increased brine volume.

The volume of brine is dependent on both temperature and salinity. As temperature decreases, more water freezes out, reducing brine volume and increasing salt concentration within the remaining brine [11]. Lower temperature restricts the movement of the ions, leading to lower dielectric loss [22]. Warmer temperatures on the other hand increase ion mobility, leading to higher dielectric losses. Higher salinity in the sea ice composite contributes to a larger brine volume, particularly during the early stages of ice formation. However, when the ice undergoes aging and other physical processes, the relationship between these two variables becomes less straightforward [20].

Additionally, research suggests that the orientation of brine inclusions within the ice matrix also affects the loss tangent [11]. A higher loss tangent is observed when brine inclusions are oriented parallel to the electric field of the electromagnetic waves, compared to when these inclusions are oriented perpendicular to the direction of the field. A higher loss tangent means greater dielectric loss and lower albedo. This orientation effect is attributed to the shape and connectivity of the brine inclusions, influencing their interaction with the electric field.

Frequency, too, affects the dielectric constant. As [21] states, the dielectric constant decreases rapidly with increasing frequency due to reduced space charge polarization (charges build up at certain areas within a material like at the boundaries between grains). When a voltage is applied, these charges can't move easily across these boundaries and pile up, causing this phenomenon. This is more pronounced at lower frequencies as the charges have more time to accumulate. However, as frequencies increase, the charges have less time to collect and the effect of space charge polarization is less pronounced, leading to a decrease in the dielectric constant. However, the author of [11] states that the dielectric constant of sea ice generally remains within 10 percent of the same value over the entire band measured, for most conditions. This suggests that in the frequency range of 26 GHz to 40 GHz, the dielectric constant of sea ice does not change significantly with increasing frequency. Though these findings may seem contrasting, they just emphasize that the frequency has stronger effects on the dielectric constant of some materials over others.

Other external factors, which do not directly relate to the structure of the sea ice have consequences too. For example, frost flowers on Arctic sea ice, as well as the thickness and structure of the ice, can have an effect. Frost flowers form when a surface brine layer on the sea ice acts as a source of water vapor that nucleates on small protrusions on the ice surface. According to [20], [22], [23], increasing the surface albedo of sea ice and due to increased brine volume increase the overall dielectric constant of the sea ice.

C. Radar Reflectivity & Satellite-Based Monitoring of Arctic Sea Ice

Before moving on to BC's effects on Radar Reflectivity, let us understand what radar reflectivity is. In simple terms, radar reflectivity is the measure of how much of the transmitted electromagnetic (EM) wave is reflected to the radar system. As discussed before, this depends on multiple factors such as the dielectric properties of materials, particle sizes, and surface characteristics. Radar reflectivity is determined by the contrast in dielectric constants between different media which in our study are sea ice and the atmosphere. The greater the contrasts in the dielectric constants, the higher the reflection coefficients [24]. This can be mathematically represented as (4).

$$\Gamma = \frac{\sqrt{\epsilon_r}-1}{\sqrt{\epsilon_r}+1} \tag{4}$$

Equation (4) determines the efficiency and proportion of radar signal reflection based on the material's dielectric properties where Γ is the radar reflectivity coefficient and ϵ_r is relative permittivity or the dielectric constant. For practical applications and standardized reporting, however, we employ decibels relative to Z (dBZ), which provides a logarithmic scale to represent radar reflectivity. The dBZ metric simplifies the interpretation of radar data by compressing a wide range of reflectivity values into a more manageable and easily comparable format [25]. This equation is shown as (5).

$$dBZ = 10 \times log_{10}(Z) \tag{5}$$

The advancements in radar reflectivity technology have made measurements more reliable and easier [26]. New models have also been able to take into account many of the environmental conditions, improving readings drastically. Despite these advancements, challenges remain in accurately capturing the contributions of small and large particles, particularly in complex atmospheric conditions like those of the Arctic, which can lead to measurement uncertainties and biases in reflectivity estimates [27]. Since BC can impact the dielectric properties of sea ice, it can also influence radar reflectivity and decrease the reflectivity coefficient.

As we've discussed before, this is disastrous: Radar reflectivity plays a crucial role in understanding various atmospheric processes in the Arctic, particularly concerning snow and cloud dynamics. The integration of ground-based and airborne radar systems allows for comprehensive assessments of snow melt, cloud microphysics, and precipitation rates [28], [29], [30]. Environmental sensing of the Arctic using these models gives us insights into global weather and climate dynamics, the accuracy of which relies heavily on radar reflectivity. Therefore, analyzing the agents

that affect radar reflectivity and subsequently environmental sensing is crucial in devising a solution to the problem.

D. Black Carbon's Impact on Electromagnetic Properties of Sea Ice & Radar Reflectivity

As mentioned before, little is known about how Black Carbon impacts the electromagnetic properties of sea ice. However, considerable research exists on the optical properties of BC and how it impacts albedo. Here, we will look into the types of BC, their distribution, their optical properties, and how they give us insights into their electromagnetic properties. Moreover, we will also talk about how BC affects communication and radar reflectivity.

Broadly, BC can be divided into two types: hydrophobic and hydrophilic. Hydrophobic black carbon reduces sea ice albedo by 0.43%, 45% larger than hydrophilic BC. As studies [18] and [31] emphasize, the smaller hydrophilic BC is more easily transported by meltwater scavenging than hydrophobic BC which further reduces its impact on albedo.

When discussing black carbon and its impact on albedo, we should note that the distribution of BC affects the level of its impact on albedo. Through meltwater scavenging, a random process depending on the porosity and percolation rates of sea ice, BC seeps into lower layers of the sea ice. As stated in [18], the surface BC will contribute more to albedo than buried BC. This tells us that a lower albedo in BC-contaminated sea ice means a higher imaginary component (ϵ'') of the dielectric constant and more energy dissipation.

As discussed in [32], the refractive index (a ratio that determines the optical properties of a material) and the dielectric constant are fundamentally related by (5) at the same frequency.

$$\kappa = n^2 \tag{6}$$

BC, which is known for its strong absorption of light, maintains a wavelength-independent refractive index across the visible spectrum [1]. A recent paper [33] has stated that the refractive index of black carbon at visible frequencies ranges from 1.75 to 1.95 for the real part, and from 0.44 to 0.79 for the imaginary part. Research [34] also describes several complexities involved in measuring the refractive index of black carbon at GHz frequencies due to irregularities, shape variability, and mixing with other compounds. Hence, the literature in that department is not abundant.

As we previously discussed, BC can hamper radar and communication signals very effectively. A main reason for this is its ability to significantly affect the attenuation of the communication signals [10]. Signal attenuation is the reduction of the amplitude of a signal, often through absorption and scattering, reducing its strength leading to poorer signal quality, higher error rates, and shorter transmission ranges. BC is very effective for this and a deeper dive into its electromagnetic properties is required to understand this behavior.

E. Conclusion of Literature review

We have at length discussed all the relevant background information for this study. In the process, we've identified several gaps of research like lack of models and values for the dielectric constant and refractive index of BC at GHz frequencies. We've also discussed reasons for this study including the dire need for improvements in climate modeling, to fill gaps in current research, and to increase environmental sensing reliability. By targeting these gaps, our research aims to advance the understanding of BC's electromagnetic properties, thereby contributing to more accurate climate predictions and more effective monitoring of Arctic environmental changes.

III. METHODOLOGY

A. Theoretical Foundation & Workflow

The theoretical foundation, mathematical equations, and parameters must be set and defined before they can be ingrained into the model. Based on the paper's hypothesis, the model will produce a table and a graph of the variation of Radar Reflectivity with BC concentration at different frequencies within the Ka-Band. There lies a lot of uncertainty in this calculation hence we must decide on the variables, parameters, and constants. The frequencies that will be used for this model in GHz are 28, 30, 32, 34, 36, 38, and 40. Note that the standard values for the speed of light c ($3 \times 10^8\ m/s$) and Permittivity of Free Space ϵ_0 ($8.85418782 \times 10^{-12}$ m^{-3} kg^{-1} s^4 A^2) will be used.

I. Sea Ice

The data for the sea ice (e.g. the dielectric constant) will be taken from already established literature [11],[35]. The dielectric properties of Arctic sea ice were determined using a swept frequency technique spanning 26.5 GHz to 40.0 GHz, which facilitated rapid and accurate data acquisition despite sample inhomogeneities. Ice samples, categorized by salinity and maintained at temperatures below -40°C, were meticulously prepared and oriented to ensure consistency during measurements. This robust methodology, detailed in [11], provides reliable dielectric constant data essential for modeling the impact of Black Carbon on radar reflectivity in Arctic sea ice. The reference includes values for the dielectric constant against frequency averaged for all salinities, temperatures, and brine orientations which will be particularly useful for this study. The research doesn't contain directly the values of the imaginary component of the dielectric constant but rather contains the values of the loss tangent and the real part of the dielectric constant of sea ice. Using (3), we can formulate Table 1.1.

TABLE I

FREQUENCY DEPENDENCE OF THE DIELECTRIC CONSTANT AND LOSS TANGENT OF SEA ICE

Frequency (GHz)	Avg. $tan\delta$	Avg. ϵ'	Avg. ϵ''
28	0.058	2.94	0.17052
30	0.060	2.98	0.17880
32	0.062	3.03	0.18786
34	0.064	3.08	0.19712
36	0.065	3.12	0.20280
38	0.067	3.17	0.21239
40	0.069	3.21	0.22149

As stated in article [35], we will use a value of 3 meters for the depth of the Arctic sea ice.

II. Black Carbon

As we've discussed before, the electromagnetic properties of black carbon are not well established. Therefore, we will use alternate mechanisms to generate accurate estimates for our model.

Though literature is available on the dielectric properties of carbon black as an additive in composites, rubbers, and plastics, the literature on black carbon aerosol, which is commonly deposited on Arctic sea ice, is limited. To estimate the real part of the dielectric constants (ϵ')of black carbon (BC) at GHz frequencies, we utilized available measurements

By leveraging the observed frequency dependence trends—where the real part (ϵ') typically decreases and the imaginary part (ϵ'') typically decreases as frequency increases [21] into the GHz range—we extrapolated BC's dielectric constants at 28, 30, 34, 36, 38, and 40 GHz. Specifically, we derived approximate ϵ' values ranging from 3.9 to 4.5, drawing on the dielectric behavior of carbonaceous materials like graphite and graphene, which are conductive and share similar structural properties with BC. Since BC is more conductive than sea ice, it has a greater ϵ' value, reflecting its higher ability to store electrical energy. The estimates were guided by the behavior of similar materials, their refractive indices as in [36], and the relationship represented in (6). Though uncertainties remain due to BC's variable structure, these estimates provide a sound basis for calculating radar reflectivity and evaluating BC's impact on sea ice dielectric properties with confidence in their scientific robustness. The estimated data is shown in Table 1.2.

TABLE II

FREQUENCY DEPENDENCE OF THE DIELECTRIC CONSTANT OF BLACK CARBON (BC)

Frequency (GHz)	Avg. ϵ' of Black Carbon
28	4.5
30	4.4
32	4.3
34	4.2
36	4.1
38	4.0
40	3.9

The calculation of the imaginary part of the dielectric constant will be done an alternate way, which is heavily reliant on existing literature and hence provides for sound estimates. Using the relationship stated in (7), we will calculate frequency depending values of ϵ''.

$$\epsilon'' = \frac{\sigma}{2\Pi f \epsilon_0} \quad (7)$$

Equation (7) specifies σ the electrical conductivity and f as the frequency. We selected an electrical conductivity value of 1 S/m for BC in our calculations based on relevant literature indicating that amorphous carbon materials, like BC, typically exhibit lower conductivity values. As noted by [37], BC contains a mixture of organic molecules and "partly graphitized solid carbon," which shares similarities with spark discharge soot. This material, with high amorphous content, has a conductivity close to 1 S/m, a reasonable estimate for BC in Arctic sea ice. This assumption aligns with the range of electrical conductivity values reported for amorphous carbon.

III. Workflow

The model will calculate the radar reflectivity for the corresponding BC concentration at each frequency listed above. For this model, we will be using concentration fractions in % as 0, 10, 20, and 30. First, the model will calculate the ϵ'_{eff} of the entire sea ice composite using the

Maxwell-Garnett Mixing Rule as used in multiple studies [38], [39], [40]. This rule allows us to calculate an effective dielectric constant that represents the composite material. This is mentioned in (8) below.

$$\epsilon'_{eff} = \epsilon'_{host}\left(\frac{\epsilon'_{inclusion} + 2\epsilon'_{host} + 2V(\epsilon'_{inclusion} - \epsilon'_{host})}{\epsilon'_{inclusion} + 2\epsilon'_{host} - V(\epsilon'_{inclusion} - \epsilon'_{host})}\right) \quad (8)$$

The ϵ'_{host} represents the real part of the dielectric constant of sea ice, the $\epsilon'_{inclusion}$ represents the real part of the dielectric constant of the BC, and the V represents the volume fraction of the BC.
Then, the model uses the frequency and electrical conductivity of BC to calculate the value of ϵ'' of BC by utilizing (7). Using the obtained the value of ϵ'' of BC and the ϵ'' of sea ice from Table 1.1, the ϵ''_{eff} of the entire composite is calculated using (8).

Next, the model calculates the combined attenuation coefficient of the sea ice - BC composite which gives us an idea of how much an electromagnetic wave is reduced in intensity as it passes through a material. We account for the combined effects by including ϵ'_{eff} in the calculation (9) written below.

$$\alpha = \frac{\omega}{c}\sqrt{\frac{\epsilon'}{2}}\left(\sqrt{1 + \left(\frac{\epsilon''}{\epsilon'}\right)^2} - 1\right)^{1/2} \quad (9)$$

Ultimately the model uses (10), a version of (5) incorporating the dielectric constant, to calculate the radar reflectivity (in dBZ) while accounting for the attenuation coefficient generated by (9).

$$dBZ = 10 \times log_{10}\left(\left(\frac{\sqrt{\epsilon'_{eff}} - 1}{\sqrt{\epsilon'_{eff}} + 1}\right)^2 . e^{-2\alpha d}\right) \quad (10)$$

Here, d represents the depth of the Arctic sea ice.

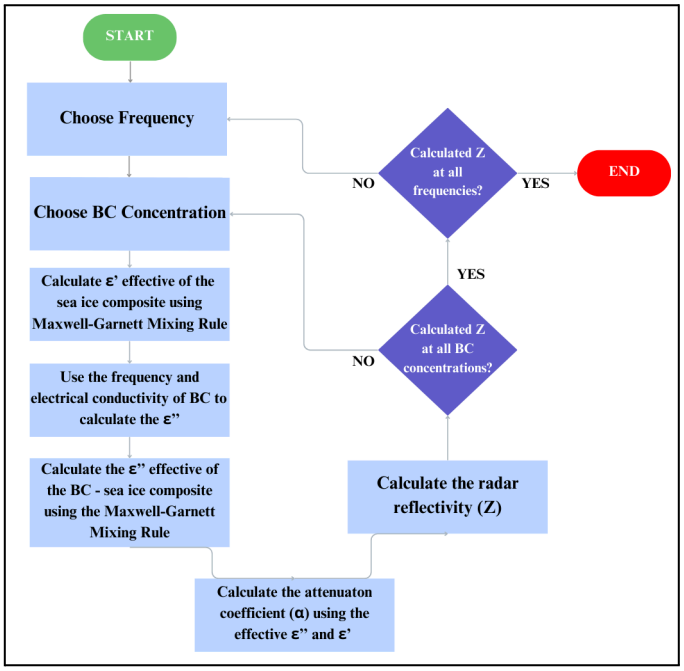

Fig. 2. This flowchart summarizes the entire workflow of the model and the steps it takes to compute radar reflectivity.

Once the values of radar reflectivity for corresponding concentrations at different frequencies are calculated, the model will generate a table representing the data calculated throughout the process and a graph plotting radar reflectivity (in dBZ) against % of black carbon concentration at all frequencies.

We acknowledge the uncertainty in the values generated by the model due to the limitations and assumptions mentioned below. Hence, to reduce the effect of this uncertainty, the model, after generating a preliminary graph and table, will generate a Monte Carlo simulation to introduce randomness in the dielectric properties and to simulate natural variability. It will perform 1000 simulations for each combination of frequency and BC concentration to get a fairer representation of the plot.

To summarize, the model will first generate a graph and table without Monte Carlo simulations which uses provided values without introducing any randomness. Second, it will generate a graph with Monte Carlo simulations to introduce randomness often observed in an environment like the Arctic. Ultimately, the third graph will average the results from the Monte Carlo simulations, accounting for the randomness, and giving a smoother curve.

B. Tools and Software

For this model, a wide array of tools were used which allowed us to collectively and efficiently compute, manage, and visualize radar reflectivity and black carbon concentration data. All the programming for this model was done in Python. We utilized several powerful tools and software within the Python programming environment. We leveraged NumPy, a

fundamental package for numerical computing, to perform array manipulations and mathematical calculations essential for our model such as the Maxwell-Garnett Mixing Rule and final Radar Reflectivity calculations. We used Pandas for managing, organizing, and handling data. To visualize the results, we employed Matplotlib which allowed us to create detailed and informative graphs of radar reflectivity against black carbon concentrations across different frequencies. Additionally, we utilized SciPy and its interpolation functions to generate smoother lines in our plots, ensuring a clear representation of the data trends. The code was executed using VSCODE, Jupyter Notebook, and Google Collabs.

C. Limits and Assumptions

In this study, we aimed to minimize assumptions and integrate all relevant factors into our model. However, given the complex interactions that happen in the Arctic, some assumptions had to be made to keep the model simpler and more accurate.

To start, (7) assumed the material to be linear and isotropic (having uniform properties in all directions). Though BC is approximately linear under typical conditions, it is generally not isotropic due to its complex particle morphology. Hence, this assumption was taken as a simplification of the model because BC's anisotropic nature could introduce complexities not captured by the model.

Equations (7) and (8) also assume the BC-sea ice composite to be a homogeneous material, that is its properties and inclusions are uniformly distributed throughout the volume. Although BC is often more concentrated at the surface, due to meltwater scavenging and other processes it does percolate to deeper layers.

Additionally, these equations also assume steady-state conditions which is a common simplification in many models. It does not fully apply to BC due to the volatile nature of the Arctic. However, it is a reasonable assumption that can be made without hampering results significantly.

The Maxwell-Garnett rule may be less accurate if the inclusions are close enough to interact. However, since BC, even when it interacts, aggregates to act as a bigger particle, this assumption does not do much harm.

The model assumes that seasonal variations do not affect the Arctic and its sea ice. However, as previously mentioned, this is not true. These variations do impact the Arctic significantly but corresponding data and literature regarding Black Carbon and sea ice in the particular seasons were not present, hence the assumption.

Other assumptions such as frequency dependence of (7), magnetic effects, and use of only low frequencies and only spherical inclusions in (8) were taken into account while developing this model.

IV. RESULTS

The following graphs (Fig. 3.1, Fig. 3.2, and Fig. 3.3) display the key outcomes of the radar reflectivity simulations as a function of black carbon concentration and frequency, based on the methodology outlined earlier. These graphs represent results without Monte Carlo, with Monte Carlo, and averaged Monte Carlo respectively.

A. Graphs and Tables

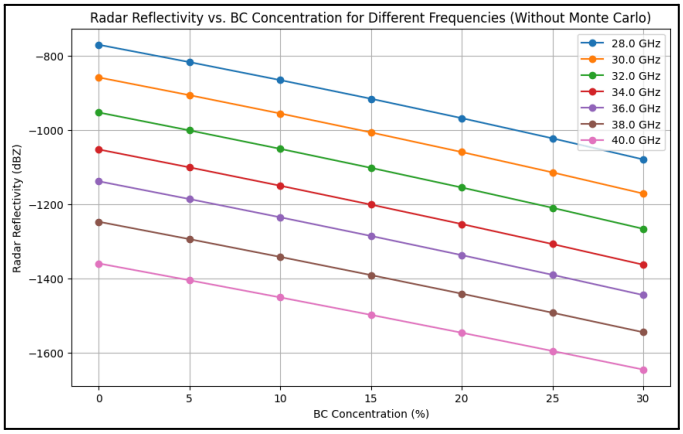

Fig. 3.1. Models Radar Reflectivity against BC concentrations at different frequencies without Monte Carlo Simulations

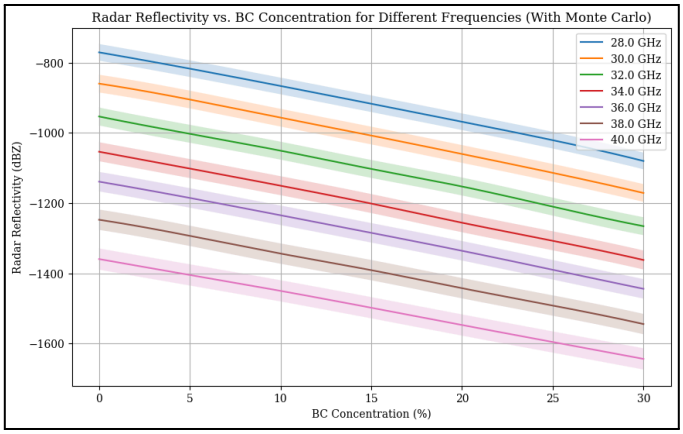

Fig. 3.2. Models Radar Reflectivity against BC concentrations at different frequencies with Monte Carlo Simulations

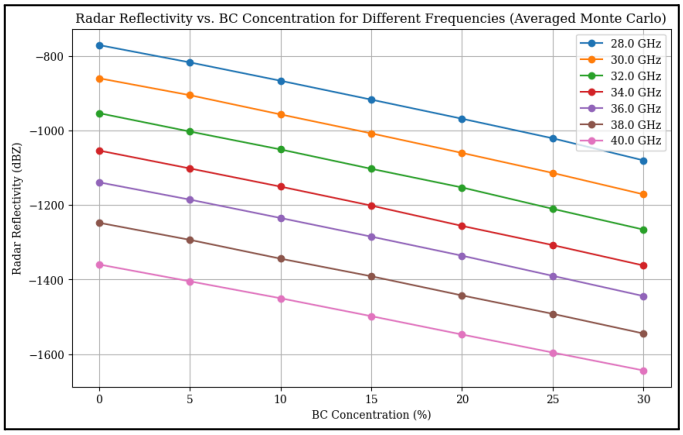

Fig 3.3. Models Radar Reflectivity against BC concentrations at different frequencies with averaged Monte Carlo Simulation values

TABLE III

CORRESPONDS TO FIG. 3.1. SPECIFIES ALL CALCULATIONS IN DETAIL

No.	Frequency (GHz)	BC Conc. (%)	Effective e'	Effective e''	Attenuation Coefficient	Radar Reflectivity (dBZ)
1	28	0	2.94	0.17052	29.147809	-771.116434
2	28	5	3.006779	0.183089	30.945426	-817.787664
3	28	10	3.074577	0.196291	32.807455	-866.142279
4	28	15	3.143418	0.210175	34.739524	-916.326666
5	28	20	3.213325	0.224795	36.747823	-968.50189
6	28	25	3.284324	0.240213	38.839184	-1022.845726
7	28	30	3.356441	0.256494	41.02117	-1079.555033
8	30	0	2.98	0.1788	32.524759	-859.008835
9	30	5	3.041691	0.190849	34.361171	-906.707857
10	30	10	3.10424	0.203451	36.257612	-955.975171
11	30	15	3.167663	0.216646	38.218858	-1006.935016
12	30	20	3.231981	0.230477	40.250118	-1059.722928
13	30	25	3.297211	0.24499	42.357088	-1114.48716
16	30	30	3.363374	0.260238	44.546014	-1171.390312
17	32	0	3.03	0.18786	36.147912	-953.294807
18	32	5	3.086059	0.199327	38.00287	-1001.49537
19	32	10	3.142814	0.21127	39.912844	-1051.132718
20	32	15	3.200278	0.22372	41.881772	-1102.309325
21	32	20	3.258464	0.23671	43.913915	-1155.136053
22	32	25	3.317386	0.250275	46.013888	-1209.733095
23	32	30	3.377058	0.264454	48.18671	-1266.231049
24	34	0	3.08	0.19712	39.970617	-1052.784649
25	34	5	3.130217	0.207937	41.822752	-1100.929371
26	34	10	3.180984	0.219157	43.72447	-1150.368556
27	34	15	3.232308	0.230803	45.678936	-1201.184573
28	34	20	3.284199	0.2429	47.689547	-1253.46582
29	34	25	3.336667	0.255474	49.759952	-1307.30733
30	34	30	3.389721	0.268554	51.894082	-1362.811446
31	36	0	3.12	0.2028	43.260623	-1138.420582
32	36	5	3.164567	0.212934	45.099673	-1186.239984
33	36	10	3.209561	0.223411	46.984057	-1235.24254
34	36	15	3.254987	0.234249	48.91638	-1285.49605
35	36	20	3.300852	0.245468	50.899419	-1337.072827
36	36	25	3.347162	0.257086	52.936141	-1390.05011
37	36	30	3.393924	0.269127	55.029718	-1444.510511
38	38	0	3.17	0.21239	47.443133	-1247.292866
39	38	5	3.208323	0.221775	49.241041	-1294.056996
40	38	10	3.246955	0.231441	51.078607	-1341.855829
41	38	15	3.285902	0.2414	52.95782	-1390.741153
42	38	20	3.325166	0.251666	54.880786	-1440.767802
43	38	25	3.364752	0.262254	56.849736	-1491.993891
44	38	30	3.404664	0.273178	58.86704	-1544.481086
45	40	0	3.21	0.22149	51.752605	-1359.498829
46	40	5	3.242301	0.230085	53.490478	-1404.713562
47	40	10	3.27482	0.238904	55.262498	-1450.819013
48	40	15	3.307558	0.247958	57.070151	-1497.853804
49	40	20	3.340519	0.257256	58.914994	-1545.85855
50	40	25	3.373703	0.266807	60.798669	-1594.875995
51	40	30	3.407114	0.276623	62.722905	-1644.95116

TABLE IV

CORRESPONDS TO FIG. 3.2. SPECIFIES ALL CALCULATIONS IN DETAIL.

No.	Frequency (GHz)	BC Conc. (%)	Effective e'	Effective e''	Attenuation Coefficient	Radar Reflectivity (dBZ)
1	28	0	2.941941	0.170689	29.170614	-771.70788
2	28	5	3.007855	0.183012	30.929932	-817.383161
3	28	10	3.072851	0.196346	32.828901	-866.70689
4	28	15	3.143497	0.209874	34.69254	-915.103756
5	28	20	3.212581	0.225179	36.817157	-970.311383
6	28	25	3.283876	0.240057	38.81893	-1022.319933
7	28	30	3.356528	0.25627	40.987256	-1078.672068
8	30	0	2.977341	0.178742	32.532081	-859.20847
9	30	5	3.043379	0.190399	34.273299	-904.415679
10	30	10	3.104975	0.203557	36.275709	-956.446705
11	30	15	3.168971	0.21677	38.235549	-1007.368344
12	30	20	3.233892	0.230123	40.179183	-1057.871565
13	30	25	3.295714	0.244724	42.323457	-1113.615086
16	30	30	3.365056	0.26044	44.572173	-1172.069582
17	32	0	3.028651	0.188193	36.2239	-955.280238
18	32	5	3.087243	0.199575	38.046065	-1002.61979
19	32	10	3.141458	0.211108	39.893828	-1050.64182
20	32	15	3.201902	0.223789	41.887172	-1102.447722
21	32	20	3.260438	0.236577	43.878745	-1154.216599
22	32	25	3.316746	0.250205	46.007872	-1209.57865
23	32	30	3.376757	0.264126	48.131903	-1264.804514
24	34	0	3.083928	0.197167	39.95923	-1052.4806
25	34	5	3.132614	0.208005	41.824231	-1100.964119
26	34	10	3.17997	0.219024	43.708014	-1149.943419
27	34	15	3.231943	0.230674	45.659252	-1200.67369
28	34	20	3.284638	0.242873	47.683936	-1253.319749
29	34	25	3.336432	0.255407	49.751211	-1307.081
30	34	30	3.389929	0.268592	51.902504	-1363.03146
31	36	0	3.122907	0.202818	43.248497	-1138.099678
32	36	5	3.162952	0.213143	45.159578	-1187.806319
33	36	10	3.210249	0.223496	47.00054	-1235.672035
34	36	15	3.252322	0.234525	48.996427	-1287.58877
35	36	20	3.299813	0.245476	50.912184	-1337.408633
36	36	25	3.349123	0.256999	52.905038	-1389.236538
37	36	30	3.392667	0.269011	55.019044	-1444.235715
38	38	0	3.171697	0.212386	47.434492	-1247.065618
39	38	5	3.208392	0.221715	49.231404	-1293.807249
40	38	10	3.247494	0.231281	51.042706	-1340.920551
41	38	15	3.288838	0.2414	52.937977	-1390.219158
42	38	20	3.326455	0.251829	54.908709	-1441.493798
43	38	25	3.366428	0.262153	56.817106	-1491.141192
44	38	30	3.404037	0.273132	58.865253	-1544.436606
45	40	0	3.211529	0.221293	51.698503	-1358.08712
46	40	5	3.241252	0.230146	53.51767	-1405.425893
47	40	10	3.27588	0.238752	55.222419	-1449.773683
48	40	15	3.309685	0.248093	57.086514	-1498.276974
49	40	20	3.339061	0.256961	58.863335	-1544.5164
50	40	25	3.372424	0.267044	60.867233	-1596.666129
51	40	30	3.406363	0.276802	62.773022	-1646.259332

B. *Analysis of Results*

Fig. 3.1 compares radar reflectivity (dBZ) across different BC concentrations and frequencies. The data reveals that as BC concentrations increase from 0% to 30%, radar reflectivity decreases substantially at all frequencies. The graph shows a decreasing, almost linear relation between reflectivity and BC concentration. It is also displayed that the lower the frequency the lower the radar reflectivity at all concentrations. However, this drop in radar reflectivity is not constant for every 2 GHz increment in frequency as the graph shows the drop between 34 GHz and 36 GHz to be visibly smaller than between any other two frequencies.

Table 2.1 corresponds to Fig. 3.1 and shows the variations of all quantities with BC concentration, not just the radar reflectivity. It can be seen that the real part of the effective dielectric constant (ϵ') for a certain frequency increases as the concentration of black carbon increases. The data also suggests that the effective dielectric constant increases as frequency is incremented. However, it is also worth noting that the effective dielectric constant of a higher frequency (e.g. 30 GHz) at a lower concentration (e.g. 0%) may be lower than the effective dielectric constant of a lower frequency (e.g. 28 GHz) at a higher concentration (e.g. 30%). The attenuation coefficient behaves similarly, increasing with increasing BC concentration and increasing frequency. This is expected as more BC would have a greater impact in lowering the amplitude of the incoming radar waves. The obtained data attests to the fact that BC has a considerable effect on reducing the accuracy and effectiveness of radar-based environmental monitoring systems.

Fig. 3.2 shows the graph as a Monte Carlo simulation which uses a probabilistic approach to run the model multiple times with varied input parameters (e.g. dielectric constant). Hence, as Fig. 3.2 shows, the data points are smoothed because of the reduced noise and uncertainties that arise from a single run of the model. The trends shown in this plot are essentially a duplicate of Fig. 3.1 but show more consistent and predictable results. This improves the reliability of the predictions.

Fig. 3.3 shows the graph as a Monte Carlo simulation with values that have been averaged to make a point simulation similar to Fig. 3.1. Though the two are almost identical, Fig. 3.3 shows a more robust representation of how Radar reflectivity varies against BC concentration at different frequencies. Expectedly, the trends are the same as Fig. 3.1 and Fig. 3.2, affirming their results. Subtle differences can be found by looking at Table 2.2 which corresponds to Fig. 3.3. Comparing the two tables, we can see a very slight difference in the Radar reflectivity values at any given frequency and BC concentration. It also appears that the difference increases as the BC concentration and the frequency increase. This differentiates the two graphs, mainly due to the reduced uncertainties in Fig. 3.3.

The results obtained agree with the hypothesis of the study which states that an increase in BC concentration deposition leads to an increase in the dielectric constant of Arctic sea ice at Ka-Band (26.5-40 GHz) frequency, leading to a decrease in radar reflectivity. All simulation plots and graphs have testified this consistently, confirming the involvement of BC in a decrease in radar reflectivity. Fig. 4 provides a simplified description of the results obtained.

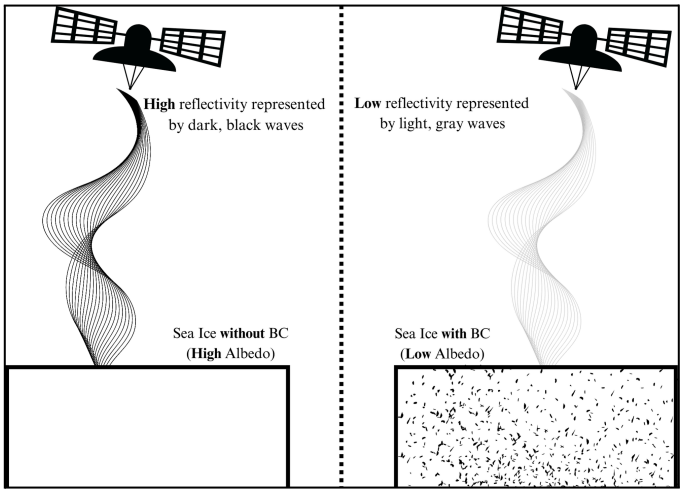

Fig. 4. A comparison of Radar Reflectivity with and without BC. As the model suggests, when concentrations of BC are present, radar reflectivity decreases.

V. DISCUSSION

The trends observed in the data highlight the impact of BC on the radar reflectivity of Arctic sea ice. As BC concentration increases, radar reflectivity consistently decreases, indicating a direct correlation between BC deposition and reduced signal strength in satellite monitoring systems operating in the Arctic. This confirms that high BC levels play a part in impairing the accuracy of climate monitoring, potentially leading to gaps in understanding critical changes in sea ice behavior. Environmental sensing, especially in the Arctic, is of high significance, and for the most accurate evaluation of global climate, the effect of BC must be accounted for. Plus, the frequency-dependent variations in radar reflectivity underscore the need for multi-band radar systems to mitigate the effects of BC interference. As BC concentrations grow due to increased biomass burning and wildfires, the effect of BC on radar reflectivity will only become more significant.

Our findings suggest that BC has broader implications on radar communication in the Arctic, something which must be mitigated to enhance the accuracy of predictions about global climate. Further research is required into the dielectric properties of BC and electromagnetic behaviors in complex interactions like meltwater scavenging and aggregation. To add, investigating the dielectric behaviors of specific types of BC (hydrophobic and hydrophilic), BC in different regions of the Arctic, and BC behaviors during different seasons is also

required to build a more comprehensive understanding of its effect on radar reflectivity.

VI. CONCLUSION

In this paper, we examined how concentrations of black carbon (BC) deposited in sea ice affect the dielectric properties and radar reflectivity of Arctic sea ice at Ka-Band frequencies. Our results indicate that higher BC concentrations significantly decrease radar reflectivity, which compromises the accuracy of satellite monitoring systems in the Arctic region. These results are vital – they emphasize the need to incorporate BC and other aerosol deposition in climate models to ensure they don't cloud the actual results or decrease accuracy.

Through further understanding of the electromagnetic behaviors and interaction of BC and its types, we will be able to enhance satellite algorithms and radar communication systems, particularly in reducing the interference caused by deposited aerosols such as BC Future research contributions should aim to understand BC's electromagnetic properties more accurately using larger models and create monitoring systems that mitigate the presence of BC in the environment as this a integral step towards advanced environmental sensing and radar technologies.

REFERENCES

[1] T. C. Bond *et al.*, "Bounding the role of black carbon in the climate system: A scientific assessment," *Journal of Geophysical Research: Atmospheres*, vol. 118, no. 11, pp. 5380–5552, Jun. 2013, doi: https://doi.org/10.1002/jgrd.50171.

[2] Z. Zhang, Z. Libo, and amp; Zhang Meigen, "A progress review of black carbon deposition on Arctic snow and ice and its impact on climate change," *Adv Polar Sci*, vol. 35, no. 2, pp. 178–191, 2024, doi: https://doi.org/10.12429/j.advps.2023.0024.

[3] F. Li *et al.*, "Arctic sea-ice loss intensifies aerosol transport to the Tibetan Plateau," *Nature Climate Change*, vol. 10, no. 11, pp. 1037–1044, Aug. 2020, doi: https://doi.org/10.1038/s41558-020-0881-2.

[4] I. H. Myers-Smith *et al.*, "Complexity revealed in the greening of the Arctic," *Nature Climate Change*, vol. 10, no. 2, pp. 106–117, Jan. 2020, doi: https://doi.org/10.1038/s41558-019-0688-1.

[5] K. von Salzen *et al.*, "Clean air policies are key for successfully mitigating Arctic warming," *Communications Earth & Environment*, vol. 3, no. 1, pp. 1–11, Oct. 2022, doi: https://doi.org/10.1038/s43247-022-00555-x.

[6] J. P. Dudley, E. P. Hoberg, E. J. Jenkins, and A. J. Parkinson, "Climate Change in the North American Arctic: A One Health Perspective," *EcoHealth*, vol. 12, no. 4, pp. 713–725, Jun. 2015, doi: https://doi.org/10.1007/s10393-015-1036-1.

[7] A. J. Parkinson and B. Evengård, "Climate change, its impact on human health in the Arctic and the public health response to threats of emerging infectious diseases," *Global Health Action*, vol. 2, no. 1, p. 2075, Nov. 2009, doi: https://doi.org/10.3402/gha.v2i0.2075.

[8] E. S. Nagovitsyna, V. A. Poddubny, A. A. Karasev, D. M. Kabanov, O. R. Sidorova, and A. S. Maslovsky, "Assessment of the Spatial Structure of Black Carbon Concentrations in the Near-Surface Arctic Atmosphere," *Atmosphere*, vol. 14, no. 1, p. 139, Jan. 2023, doi: https://doi.org/10.3390/atmos14010139.

[9] Nobuhiro Moteki, "Correction: Climate-relevant properties of black carbon aerosols revealed by in situ measurements: a review," *Progress in Earth and Planetary Science*, vol. 10, no. 1, Mar. 2023, doi: https://doi.org/10.1186/s40645-023-00546-2.

[10] X. Zhang, X. Tan, M. Zhai, and L. Zhou, "Influence of Soot Aerosol on Satellite-ground Quantum Communication Performance," *Research Square (Research Square)*, Feb. 2022, doi: https://doi.org/10.21203/rs.3.rs-630551/v1.

[11] R. Byrd, "THE DIELECTRIC PROPERTIES OF SEA ICE IN THE FREQUENCY RANGE FROM 26GHz to 40GHz," Thesis (M.S.), University of Alaska Fairbanks, 1971.

[12] X. Zhu, T. J. Pasch, M. A. Ahajjam, and A. Bergstrom, "Environmental Monitoring for Arctic Resiliency and Sustainability: An Integrated Approach with Topic Modeling and Network Analysis," *Sustainability*, vol. 14, no. 24, p. 16493, Dec. 2022, doi: https://doi.org/10.3390/su142416493.

[13] Balint Alfoldy, Asta Gregorič, Matic Ivančič, I. Ježek, and M. Rigler, "Source apportionment of black carbon and combustion-related CO_2 for the determination of source-specific emission factors," *Atmospheric measurement techniques*, vol. 16, no. 1, pp. 135–152, Jan. 2023, doi: https://doi.org/10.5194/amt-16-135-2023.

[14] S. Eckhardt *et al.*, "Sources and seasonality of black carbon in Europe," Mar. 2024, doi: https://doi.org/10.5194/egusphere-egu24-7993.

[15] R. Srivastava and M. Ravichandran, "Spatial and seasonal variations of black carbon over the Arctic in a regional climate model," *Polar Science*, vol. 30, p. 100670, Dec. 2021, doi: https://doi.org/10.1016/j.polar.2021.100670.

[16] Black, "WHAT IS BLACK CARBON?," 2010.

[17] M. T. Lund *et al.*, "Short Black Carbon lifetime inferred from a global set of aircraft observations," *npj Climate and Atmospheric Science*, vol. 1, no. 1, Oct. 2018, doi: https://doi.org/10.1038/s41612-018-0040-x.

[18] C. Jiao *et al.*, "An AeroCom assessment of black carbon in Arctic snow and sea ice," *Atmospheric Chemistry and Physics*, vol. 14, no. 5, pp. 2399–2417, Mar. 2014, doi: https://doi.org/10.5194/acp-14-2399-2014.

[19] D. Archer and V. Brovkin, "The millennial atmospheric lifetime of anthropogenic CO2," *Climatic Change*, vol. 90, no. 3, pp. 283–297, Jun. 2008, doi: https://doi.org/10.1007/s10584-008-9413-1.

[20] J. K. Ehn, B. J. Hwang, R. Galley, and D. G. Barber, "Investigations of newly formed sea ice in the Cape Bathurst polynya: 1. Structural, physical, and optical properties," *Journal of Geophysical Research Atmospheres*, vol. 112, no. C5, Apr. 2007, doi: https://doi.org/10.1029/2006jc003702.

[21] Ch. Rayssi, S. El.Kossi, J. Dhahri, and K. Khirouni, "Frequency and temperature-dependence of dielectric permittivity and electric modulus studies of the solid solution $Ca_{0.85}Er_{0.1}Ti_{1-x}Co_{4x/3}O_3$ ($0 \leq x \leq 0.1$)," *RSC Advances*, vol. 8, no. 31, pp. 17139–17150, 2018, doi: https://doi.org/10.1039/c8ra00794b.

[22] D. K. Perovich, "Seasonal changes in sea ice optical properties during fall freeze-up," *Cold Regions Science and Technology*, vol. 19, no. 3, pp. 261–273, Aug. 1991, doi: https://doi.org/10.1016/0165-232x(91)90041-e.

[23] D. K. Perovich, "Complex yet translucent: the optical properties of sea ice," *Physica B: Condensed Matter*, vol. 338, no. 1–4, pp. 107–114, Oct. 2003, doi: https://doi.org/10.1016/s0921-4526(03)00470-8.

[24] N. A. Ismail, N. Mohd Muztaza, and R. Saad, "REFLECTIVITY OF ELECTROMAGNETIC (EM) WAVE IN SHALLOW GROUND PENETRATING RADAR (GPR) SURVEY," *Jurnal Teknologi*, vol. 78, no. 7–3, Jul. 2016, doi: https://doi.org/10.11113/jt.v78.9500.

[25] W. Keat, "Novel Applications of Polarimetric Radar in Mixed-Phase Clouds and Rainfall," Thesis (PhD), UNIVERSITY OF READING Department of Meteorology, 2006.

[26] E. N. Anagnostou and W. F. Krajewski, "Simulation of radar reflectivity fields: Algorithm formulation and evaluation," *Water resources research*, vol. 33, no. 6, pp. 1419–1428, Jun. 1997, doi: https://doi.org/10.1029/97wr00233.

[27] D. Atlas, "Advances in Radar Meteorology," *Elsevier eBooks*, pp. 317–478, Jan. 1964, doi: https://doi.org/10.1016/s0065-2687(08)60009-6.

[28] J.-M. Friedt, É. Bernard, and M. Griselin, "Ground-Based Oblique-View Photogrammetry and Sentinel-1 Spaceborne RADAR Reflectivity Snow Melt Processes Assessment on an Arctic Glacier," *Remote Sensing*, vol. 15, no. 7, p. 1858, Mar. 2023, doi: https://doi.org/10.3390/rs15071858.

[29] C. M. Nguyen *et al.*, "Coincident In-situ and Triple-Frequency Radar Airborne Observations in the Arctic," *OPAL (Open@LaTrobe) (La Trobe University)*, Jul. 2021, doi: https://doi.org/10.5194/amt-2021-148.

[30] M. Oue, M. Galletti, J. Verlinde, A. Ryzhkov, and Y. Lu, "Use of X-Band Differential Reflectivity Measurements to Study Shallow Arctic Mixed-Phase Clouds," *Journal of Applied Meteorology and Climatology*, vol. 55, no. 2, pp. 403–424, Feb. 2016, doi: https://doi.org/10.1175/jamc-d-15-0168.1.

[31] Y. Wang and J. Su, "Sensitivity study of the effects of black carbon on Arctic sea ice using CICE sea-ice model," Feb. 2023, doi: https://doi.org/10.5194/egusphere-egu23-10572.

[32] B. Smith, "Relation of the Dielectric Constant and the Refractive Index to Thermodynamic Properties."

[33] R. A. R. Digby, K. von Salzen, A. H. Monahan, N. P. Gillett, and J. Li, "The impact of uncertainty in black carbon's refractive index on simulated optical depth and radiative forcing," Jun. 2024, doi: https://doi.org/10.22541/essoar.171805223.31837756/v1.

[34] Nobuhiro Moteki, S. Ohata, A. Yoshida, and K. Adachi, "Constraining the complex refractive index of black carbon particles using the complex forward-scattering amplitude," *Aerosol Science and Technology*, vol. 57, no. 7, pp. 678–699, Apr. 2023, doi: https://doi.org/10.1080/02786826.2023.2202243.

[35] National Snow and Ice Data Center, "Sea Ice," *National Snow and Ice Data Center*. https://nsidc.org/learn/parts-cryosphere/sea-ice

[36] Nobuhiro Moteki, "Climate-relevant properties of black carbon aerosols revealed by in situ measurements: a review," *Progress in Earth and Planetary Science*, vol. 10, no. 1, Mar. 2023, doi: https://doi.org/10.1186/s40645-023-00544-4.

[37] M. Moalleminejad and D. D. L. Chung, "Dielectric constant and electrical conductivity of carbon black as an electrically conductive additive in a manganese-dioxide electrochemical electrode, and their dependence on electrolyte permeation," *Carbon*, vol. 91, pp. 76–87, Sep. 2015, doi: https://doi.org/10.1016/j.carbon.2015.04.047.

[38] P. Mallet, Charles-Antoine Guérin, and A. Sentenac, "Maxwell-Garnett mixing rule in the presence of multiple scattering: Derivation and accuracy," *Physical Review B*, vol. 72, no. 1, Jul. 2005, doi: https://doi.org/10.1103/physrevb.72.014205.

[39] M. Y. Koledintseva, R. E. DuBroff, and R. W. Schwartz, "MAXWELL GARNETT RULE FOR DIELECTRIC MIXTURES WITH STATISTICALLY DISTRIBUTED ORIENTATIONS OF INCLUSIONS," *Progress In Electromagnetics Research*, vol. 99, pp. 131–148, 2009, doi: https://doi.org/10.2528/pier09091605.

[40] D. T. Meiers and Georg von Freymann, "Mixing rule for calculating the effective refractive index beyond the limit of small particles," *Optics Express*, vol. 31, no. 20, pp. 32067–32067, Jul. 2023, doi: https://doi.org/10.1364/oe.494653.